IEEE Access
Multidisciplinary | Rapid Review | Open Access Journal

Received July 8, 2021, accepted July 12, 2021, date of publication July 15, 2021, date of current version July 23, 2021.

Digital Object Identifier 10.1109/ACCESS.2021.3097378

Adaptive Deadbeat Predictive Current Control for PMSM With Feed Forward Method

KAIXUAN YIN[1], LIN GAO[1], RUI CHEN[2], ZHIYU FENG[1], AND SHEN LIU[1]
[1]Institute of Electrical Machine and All-Electric Technology, Xi'an Jiaotong University, Xi'an 710049, China
[2]School of Electrical Engineering, Southeast University, Nanjing 210096, China

Corresponding author: Kaixuan Yin (ykx199717@163.com)

ABSTRACT The steady-state error and torque ripple caused by the mismatch or variation of parameters in the deadbeat predictive current control of permanent magnet synchronous motor are presented in this paper. An improved adaptive deadbeat current predictive model only related to inductance parameters is proposed. The influence of inductance variation on the system stability margin is quantitatively analyzed. When the variation is less than 50%, the system performance can be improved obviously. When the variation reaches 50%, the system will oscillate and cannot operate stably. The feed forward control strategy is introduced to improve the stability margin of the system, and the inductance disturbance of the system oscillation is expanded to 67%. Simulations and experiments are carried out for traditional deadbeat current predictive model, adaptive deadbeat predictive model, and adaptive model with feed forward control. Results show that under various working conditions, the effectiveness of the proposed method in eliminating the steady-state error caused by parameter disturbances is verified. The current distortion and torque ripple are also restrained. Both robustness and steady-state performance of the system are improved.

INDEX TERMS Permanent magnet synchronous motor (PMSM), stability margin, deadbeat predictive current control (DPCC), parameter mismatch, feed forward control, steady-state performance.

I. INTRODUCTION

Permanent magnet synchronous motor (PMSM) has been widely used in the military industry and national defense for advantages of small volume and high efficiency. PI control is widely used among various control algorithms in vector control systems, which is easy to realize but limited by large overshoot and difficulty in precise adjustment of parameters.

Based on rigorous mathematical derivation, model predictive control (MPC) can achieve minor steady-state response error and flexible control of multiple variables [1]–[3]. The traditional finite control set MPC uses a cost function to uniquely determine the output voltage vector by predicting the current in variable switching states. The accuracy of the control system depends on the complexity of cost function. When this method is applied to the control system, problems such as large stator current distortion and complicated calculation will be caused. In [4], from the perspective of duty cycle modulation, a low-complexity MPC was presented. The computation burden and execution time were both reduced, excellent steady-state performance and quick dynamic response were also achieved. Aiming at the large torque ripple and current distortion rate in MPC, a brand-new compensation technique based on dual sampling within a control period was proposed. The novel delay compensation scheme was composed of two sequential procedures. The torque ripple was decreased by 8% after compensation [5].

The dynamic performance of traditional finite control set MPC is inferior because of unfixed control frequency. Deadbeat predictive current control (DPCC) is combined with SVPWM modulation technology, with a fixed control frequency, good current dynamic performance, and small current ripple, which has been adopted in many industrial fields [6], [7]. However, the control accuracy of deadbeat predictive current control depends on the mathematical model of PMSM. Response error will be caused when machine parameter deviations from nominal ones or lack of knowledge of their values [8]. Aiming at the problem caused by unknown parameters, finite element analysis could be used to derive the initial values of dq-axis inductances. The flux linkage of the motor was calculated based on the back EMF [9]. This method could effectively avoid the parameter mismatch by measuring the nominal values of the motor accurately.

The parameters will also change due to the magnetic saturation and cross-coupling during the operation of the motor. Aiming at the disturbance caused by parameter changes,

The associate editor coordinating the review of this manuscript and approving it for publication was Shihong Ding.

in [10], an accurate deadbeat control method was proposed based on the exact model of PMSM in a stationary two-phase frame with a moving horizon estimator. The control algorithm was simplified, and the sensitivity of the system to the parameters was reduced. In [11], the complex magnetic phenomena have been considered. A methodology based on finite element methods was suggested to incorporate the direct and cross-saturation effects into the deadbeat control routine. The deadbeat controller performed satisfactorily under steady-state and transient conditions. In [12], a deadbeat PI controller was proposed by modifying the feed forward. With the modified feed forward, the dynamic performance and harmonic suppression ability of the system can be ensured when faced with parameter mismatch. The disturbance overshoot was reduced by 20% compared with the conventional method. In [13]–[19], the disturbance observers were designed in DPCC to eliminate the steady-state error of current and a lower computation burden was achieved. In [20], instead of using observer-based disturbance voltage feed forward methods, a new closed-form strategy was proposed to directly compensate the current tracking errors with a simple feed forward term, whose computation is negligible compared to the observer-based methods. In [21]–[23], the parameter identification algorithms were introduced into the DPCC. The identified parameters were brought into the predictive model in real time, trying to fundamentally eliminate the error. However, the complexity of algorithms was greatly increased, and the convergence of the algorithms also took a certain amount of time, making it impossible to eliminate errors in real time.

In this paper, an improved deadbeat predictive current control strategy is designed for surface-mounted permanent magnet synchronous motor (SPMSM) to solve the problems of control accuracy degradation and steady-state error when there is parameter mismatch in the traditional DPCC algorithm. Different from the previous strategy, which proposed a new active disturbance rejection scheme with a second-order variable speed sliding mode observer to eliminate the steady-state error [24], this paper takes the optimization of predictive algorithm as the breakthrough point for SPMSM. An adaptive DPCC model is proposed, which greatly reduces the complexity of the system and further improves the control effect. The resistance voltage drop, back electromotive force, and voltage error caused by parameter disturbance are all regarded as disturbance terms and then predicted in the proposed algorithm. The steady-state error of current caused by parameter disturbance, especially inductance mismatch, is eliminated completely. The improved adaptive predictive algorithm eliminates the influence of resistance and flux linkage disturbance, and the control performance is only related to inductance. When the inductance mismatch is less than 50%, the performance of the system is improved obviously. When the mismatch reaches 50%, the system oscillates violently and cannot meet the accuracy requirements. In order to solve the problems of the improved strategy, the feed forward control strategy is further introduced into the adaptive DPCC. The proposed method can eliminate the steady-state error of current and increase the stability margin of the system, which will increase the inductance disturbance momentum to 67%. The anti-jamming ability and dynamic performance of the system are also improved.

II. CONVENTIONAL DEADBEAT PREDICTIVE MODEL

A. MACHINE MODEL OF SPMSM

The state equations of SPMSM in synchronous rotating coordinate system can be expressed as follows

$$\begin{cases} L\dfrac{\mathrm{d}i_d}{\mathrm{d}t} = -R_s \cdot i_d + L\omega_e i_q + u_d \\ L\dfrac{\mathrm{d}i_q}{\mathrm{d}t} = -R_s \cdot i_q - L\omega_e i_d + u_q - \psi_{\mathrm{f}}\omega_e \end{cases} \tag{1}$$

The motion equation of SPMSM is given as

$$T_e = T_L + \frac{B}{P_n}\omega_e + \frac{J}{P_n} \cdot \frac{\mathrm{d}\omega_e}{\mathrm{d}t} \tag{2}$$

where i_d and i_q represent current of d-q axis, respectively, u_d and u_q represent voltage of d-q axis, respectively, R_s represents stator resistance, ω_e represents electrical angular velocity, L represents inductance of d-q axis, ψ_{f} represents permanent magnet flux linkage, B represents the damping coefficient, T_L represents the load torque converted to the motor shaft end, J represents the moment of inertia, and P_n represents the number of pole pairs.

B. CONVENTIONAL PREDICTIVE MODEL OF DPCC

The Euler method is used to discretize the state equations of SPMSM. Define the sampling period as T, and the discretized model is obtained as

$$i(k+1) = A(k) \cdot i(k) + G \cdot U(k) + d(k) \tag{3}$$

where

$$i(k) = \begin{bmatrix} i_d(k) \\ i_q(k) \end{bmatrix}, \quad G = \begin{bmatrix} \dfrac{T}{L} & 0 \\ 0 & \dfrac{T}{L} \end{bmatrix}, \quad U(k) = \begin{bmatrix} u_d(k) \\ u_q(k) \end{bmatrix},$$

$$d(k) = \begin{bmatrix} 0 & \dfrac{-T\psi_{\mathrm{f}}\omega_e(k)}{L} \end{bmatrix}^{\mathrm{T}},$$

$$A(k) = \begin{bmatrix} 1 - \dfrac{TR_s}{L} & T\omega_e(k) \\ -T\omega_e(k) & 1 - \dfrac{TR_s}{L} \end{bmatrix}$$

Take the given current $i^*(k)$ as the predictive current $i(k+1)$. According to equation (3), the predictive current and the feedback current are both taken as inputs to calculate the voltage vector, which will be modulated by SVPWM to obtain the desired stator voltage, and then the switching sequence of the inverter is determined. Figure 1 is the control block diagram of DPCC.

It can be seen from equation (3) that the performance of current controller depends on the motor parameters. If the values used by the controller and the actual parameters of

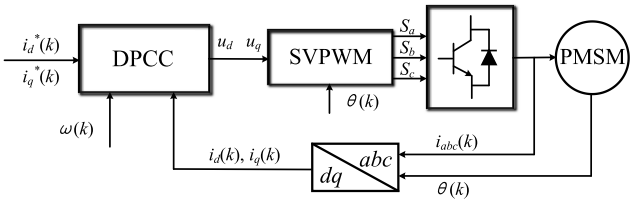

FIGURE 1. Control block diagram of DPCC.

SPMSM are mismatched, current distortion and electromagnetic torque instability will be caused. Since the disturbance caused by the motor resistance can be ignored, assuming that R_s is constant, the voltage equations of conventional DPCC are expressed as follows

$$\begin{cases} u_d(k) = \dfrac{L}{T} i_d^*(k) + (R_s - \dfrac{L}{T}) i_d(k) - \omega_e(k) L i_q(k) \\ u_q(k) = \dfrac{L}{T} i_q^*(k) + (R_s - \dfrac{L}{T}) i_q(k) + \omega_e(k) L i_d(k) \\ \qquad + \omega_e(k) \psi_f \end{cases} \tag{4}$$

When the inductance and flux linkage of SPMSM change, the voltage equations after disturbance can be rewritten as

$$\begin{cases} u_d(k) = \dfrac{L'}{T} i_d(k+1) + (R_s - \dfrac{L'}{T}) i_d(k) - \omega_e(k) L' i_q(k) \\ u_q(k) = \dfrac{L'}{T} i_q(k+1) + (R_s - \dfrac{L'}{T}) i_q(k) + \omega_e(k) L' i_d(k) \\ \qquad + \omega_e(k) \psi_f' \end{cases} \tag{5}$$

where L' represents the actual inductance of SPMSM during operation, ψ_f' represents the actual flux linkage of permanent magnet.

In the case of steady-state, it can be approximately considered that

$$\begin{aligned} i_d(k+1) = i_d(k) = i_d(k-1), i_d^*(k) = i_d^*(k-1) \\ i_q(k+1) = i_q(k) = i_q(k-1), i_q^*(k) = i_q^*(k-1) \end{aligned} \tag{6}$$

By subtracting equation (4) from equation (5), the steady-state error between the feedback current and the given current can be obtained as

$$\begin{aligned} \Delta i_d^*(k) &= \frac{T}{L} \omega_e(k) \Delta L i_q(k) \\ \Delta i_q^*(k) &= \frac{T}{L} \omega_e(k) [\Delta L i_d(k) + \Delta \psi_f] \end{aligned} \tag{7}$$

where ΔL is the inductance deviation and $\Delta\psi_f$ is the flux linkage deviation, $\Delta i_d^*(k) = i_d^*(k) - i_d(k)$ and $\Delta i_q^*(k) = i_q^*(k) - i_q(k)$ are steady-state errors of the dq-axis current, respectively.

For traditional DPCC, the SPMSM adopts $i_d = 0$ control method. It can be seen from equation (7) that when the inductance and the flux linkage are disturbed, the steady-state error of the dq-axis current will be caused, respectively. Therefore, it is necessary to optimize the predictive model to enhance the robustness of the system.

III. ADAPTIVE DEADBEAT PREDICTIVE MODEL

A. ESTABLISHMENT OF ADAPTIVE MODEL

Considering the voltage error caused by parameter mismatch, the state equations in equation (3) can be further expressed as

$$\begin{cases} i_d(k+1) = i_d(k) + \dfrac{T}{L}(u_d(k) - R_s i_d(k) \\ \qquad + \omega_e L i_q(k)) - v_d \\ i_q(k+1) = i_q(k) + \dfrac{T}{L}(u_q(k) - R_s i_q(k) - \omega_e L i_d(k) \\ \qquad - \omega_e \psi_f) - v_q \end{cases} \tag{8}$$

where v_d and v_q are the voltage errors caused by the mismatch or change of dq-axis parameters, respectively.

The resistance voltage drop $R_s i(k)$, back electromotive force $\omega_e\psi_f$, voltage error term v_d, v_q, and other voltage control variables that cause current disturbance are all regarded as disturbance terms, which are converted into the online estimation of e_d and e_q. The equation (8) can be rewritten as

$$\begin{cases} i_d(k+1) = i_d(k) + \dfrac{T}{L}[u_d(k) - e_d(k)] \\ i_q(k+1) = i_q(k) + \dfrac{T}{L}[u_q(k) - e_q(k)] \end{cases} \tag{9}$$

Since the values of voltage disturbance terms (e_d and e_q) are related to the steady-state error of current. The derivatives of disturbance terms to time are

$$\begin{cases} \dfrac{de_d}{dt} = \dfrac{e_d(k+1) - e_d(k)}{T} = k_d[i_d(k) - i_d^*(k)] \\ \dfrac{de_q}{dt} = \dfrac{e_q(k+1) - e_q(k)}{T} = k_q[i_q(k) - i_q^*(k)] \end{cases} \tag{10}$$

The following predictive equations are obtained

$$\begin{cases} e_d(k+1) = e_d(k) - T \cdot k_d[i_d(k) - i_d^*(k)] \\ e_q(k+1) = e_q(k) - T \cdot k_q[i_q(k) - i_q^*(k)] \end{cases} \tag{11}$$

where $e_d\ (k+1)$ and $e_q\ (k+1)$ are the predicted values of voltage disturbance terms at the $(k+1)$ sequence. k_d and k_q are the gain coefficients of the predictive equations, which determine the rate that the prediction term approaches stability.

The control model of adaptive DPCC is composed of equation (9) and equation (11). When the actual value of current cannot follow the given value, there is a steady-state error. According to equation (11), the voltage disturbance terms at the next sequence will increase. In equation (9), the increase of voltage disturbance terms will make the actual current quickly approach the given value. The system will gradually stabilize. In steady-state, $e_d(k) = u_d(k)$, $e_q(k) = u_q(k)$.

B. PARAMETER SENSITITY OF ADAPTIVE MODEL

Firstly, the stability margin of the predictive model is analyzed quantitatively. The control strategy of $i_d = 0$ is adopted to simplify the state equations of the system. The adaptive deadbeat predictive model is not affected by R_s and ψ_f.

This paper only analyzes the influence of inductance mismatch. In steady-state, the variations of voltage disturbance terms can be ignored. According to equation (9), the voltage equations of q axis before and after inductance disturbance can be written as

$$\begin{cases} u_q(k) = \dfrac{L}{T}[i_q^*(k) - i_q(k)] + e_q(k) \\ u_q(k) = \dfrac{L'}{T}[i_q(k+1) - i_q(k)] + e_q(k) \end{cases} \tag{12}$$

where L' is the actual inductance.

Subtract the two formulas, and the error is obtained as follows

$$\frac{L}{T}i_q^*(k) - \frac{L'}{T}i_q(k+1) + \frac{L'-L}{T}i_q(k) = 0 \tag{13}$$

The equation (13) is discretized in the Z domain and expressed as

$$Li_q^*(z) - L'zi_q(z) + (L'-L)i_q(z) = 0 \tag{14}$$

Then the transfer function is obtained as

$$\frac{i_q(z)}{i_q^*(z)} = \frac{L/L'}{z + (L/L') - 1} \tag{15}$$

Therefore, the pole $z = 1-L/L'$ is obtained. Since the voltage equations of the adaptive predictive model are consistent with the traditional DPCC, under the two predictive algorithms, analysis shows that when $L' \leq L/2$, current oscillation or divergence will be caused.

The steady-state performance of the system is further analyzed quantitatively. The voltage equations before and after the inductance disturbance are as follows

$$\begin{cases} u_d(k) = \dfrac{L}{T}i_d^*(k) - \dfrac{L}{T}i_d(k) + e_d(k) \\ u_q(k) = \dfrac{L}{T}i_q^*(k) - \dfrac{L}{T}i_q(k) + e_q(k) \end{cases} \tag{16}$$

$$\begin{cases} u_d(k) = \dfrac{L'}{T}i_d(k+1) - \dfrac{L'}{T}i_d(k) + e'_d(k) \\ u_q(k) = \dfrac{L'}{T}i_q(k+1) - \dfrac{L'}{T}i_q(k) + e'_q(k) \end{cases} \tag{17}$$

Subtract equation (17) from equation (16). With the introduction of equation (6), the error is simplified as

$$\begin{cases} \Delta i_d^*(k) = \dfrac{T}{L}\Delta e_d(k) \\ \Delta i_q^*(k) = \dfrac{T}{L}\Delta e_q(k) \end{cases} \tag{18}$$

where $\Delta e_d(k) = e_d(k) - e'_d(k)$ and $\Delta e_q(k) = e_q(k) - e'_q(k)$ are the variations of voltage disturbances at the current sequence.

When the system is stable, $e_d(k) = e'_d(k) = u_d(k)$, $e_q(k) = e'_q(k) = u_q(k)$, and the voltage disturbances approach zero. According to equation (18), the steady-state error of current can be eliminated.

It can also be seen from equation (9) that the improved predictive model is only related to the inductance of SPMSM, eliminating the dependence on other parameters. When the inductance is disturbed, to eliminate the steady-state error of the current in real time, larger approach coefficients k_d and k_q must be adopted to make the voltage disturbance item quickly stabilize. A more significant approach rate will also aggravate the chattering of the system. As shown in equation (15), when the inductance disturbance reaches half of the nominal inductance, the system oscillates violently, and the dynamic performance cannot meet the requirements.

IV. ADAPTIVE DPCC COMBINED WITH FEED FORWARD CONTROL

A. MODEL WITH FEED FORWARD CONTROL

Although the adaptive model is no longer affected by the variation of motor resistance and flux linkage, it still depends on the inductance of SPMSM. If the error between the value of controller and the actual inductance reaches 50%, the current will vibrate violently, and the unstable electromagnetic torque will be output. To further improve the allowable range of inductance error for system stability, the feed forward variable $i^*(k-1)$ is introduced to revise the feedback current.

The state equations after introducing feed forward control are as follows

$$\begin{cases} i_d(k+1) = i_{Fd}(k) + \dfrac{T}{L}[u_d(k) - e_d(k)] \\ i_q(k+1) = i_{Fq}(k) + \dfrac{T}{L}[u_q(k) - e_q(k)] \end{cases} \tag{19}$$

where $i_{Fd}(k)$ and $i_{Fq}(k)$ represent the corrected current of dq-axis, which are used to replace the feedback current $i_d(k)$ and $i_q(k)$.

Suppose the weight of feed forward is q, and $0 < q < 1$, the expression of $i_F(k)$ can be obtained as

$$i_F(k) = qi(k) + (1-q)i^*(k-1) \tag{20}$$

Figure 2 is the block diagram of adaptive DPCC control system with feed forward control. Compared with figure 1, it can be seen that the traditional DPCC is replaced by the adaptive predictive model, and the feed forward component of current is introduced into the input of adaptive model.

As can be seen from Figure 2, when the weight value $q = 0$, the current controller adopts feed forward control. When $q = 1$, it is adaptive deadbeat predictive current control. The feed forward control directly invokes the current command through the running state of the motor, while the predictive control adjusts the current through the feedback

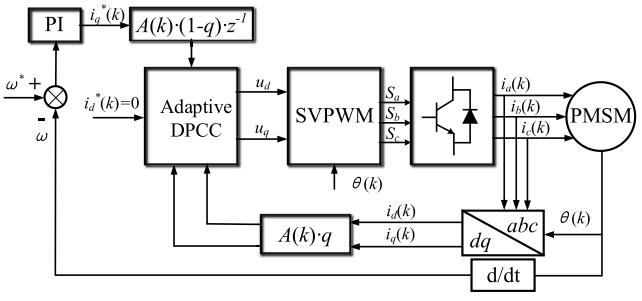

FIGURE 2. Adaptive deadbeat control with feed forward.

voltage vector. Reasonable selection of q can effectively reduce the influence of parameter disturbance on the system, decrease the current distortion and torque ripple, and improve the robustness of SPMSM control system.

B. SENSITIVITY ANALYSIS

The steady-state error of current after inductance disturbance is quantitatively analyzed to determine the value of weight q. For the adaptive DPCC combined with feed forward control, the voltage equations before and after the inductance disturbance are obtained, respectively.

$$\begin{cases} u_d(k) = \dfrac{L}{T} i_d^*(k) - \dfrac{L}{T} i_{Fd}(k) + e_d(k) \\ u_q(k) = \dfrac{L}{T} i_q^*(k) - \dfrac{L}{T} i_{Fq}(k) + e_q(k) \end{cases} \tag{21}$$

$$\begin{cases} u_d(k) = \dfrac{L'}{T} i_d(k+1) - \dfrac{L'}{T} \cdot i_{Fd}(k) + e'_d(k) \\ u_q(k) = \dfrac{L'}{T} i_q(k+1) - \dfrac{L'}{T} \cdot i_{Fq}(k) + e'_q(k) \end{cases} \tag{22}$$

Subtract equation (22) from equation (21), and the error is obtained as

$$\frac{L - (1-q)\Delta L}{T} \cdot i^*(k) - \frac{L' + q\Delta L}{T} i(k) + \Delta e(k) = 0 \tag{23}$$

where $i^*(k) = [i_d^*(k), i_q^*(k)]$, $i(k) = [i_d(k), i_q(k)]$. ΔL is the error between the nominal inductance and the actual inductance.

Only when $q = 0.5$, the coefficients of $i^*(k)$ and $i(k)$ in equation (23) are equal. The following equation holds

$$\frac{L - 0.5\Delta L}{T} = \frac{L' + 0.5\Delta L}{T} = \frac{0.5L + 0.5L'}{T} \tag{24}$$

It can be seen from equation (23) that since $\Delta e(k)$ is zero in the steady-state, the adaptive DPCC with feed forward control can ensure that the steady-state error of current will equal to zero when the inductance is mismatched.

In the steady-state, the variation of voltage disturbance term is ignored. The stability margin of the system is analyzed quantitatively. The voltage equations of q axis before and after inductance disturbance can be written as

$$\begin{cases} u_q(k) = \dfrac{L}{T}\left[i_q^*(k) - i_{F_q}(k)\right] + e_q(k) \\ u_q(k) = \dfrac{L'}{T}\left[i_q(k+1) - i_{F_q}(k)\right] + e_q(k) \end{cases} \tag{25}$$

Subtract the two formulas, and the error is as follows

$$\frac{L}{T} i_q^*(k) - \frac{\Delta L}{T}(1-q) i_q^*(k-1) = \frac{L'}{T} i_q(k+1) + \frac{\Delta L}{T} q i_q(k) \tag{26}$$

Equation (26) can be rewritten into the format of Z function as

$$\frac{i_q(z)}{i_q^*(z)} = \frac{L - \Delta L(1-q)z^{-1}}{L'z + \Delta L q} \tag{27}$$

The pole obtained from Equation (27) is $z = q(1-L/L')$. Since q is fixed to 0.5, the operating point of oscillation is reduced to 1/3 of the nominal inductance. The stability margin of the system to inductance is increased to ensure that the motor can still run stably under extreme parameter mismatch conditions.

To sum up, the adaptive DPCC with feed forward control strategy is proposed. When the inductance is mismatched, on the basis of eliminating the steady-state error, the robustness of the system to inductance is improved. The inductance disturbance momentum of the system is increased from 50% to 67%.

V. SIMULATION AND EXPERIMENT RESULTS

To explore the performance of the system under the proposed control strategy, the nominal parameters of the SPMSM used in the simulation and experiment are shown in Table 1. The sampling period T of the system is 100μs, and the approach coefficients k_d, k_q in the voltage disturbance term are 20000, respectively. The value of weight q is 0.5.

TABLE 1. Main parameters of SPMSM.

Items	Value	Items	Value
R_s (Ω)	0.201	Ψ_f (Wb)	0.246
L_d (mH)	1.576	Moment of Inertia (kg·m^2)	0.003
L_q (mH)	1.576	Rated Power (kW)	3.1
Poles	3	Rated Speed (r·min^{-1})	2000
Rated Current (A)	12.476	Rated Torque (N·m)	14.8

A. SIMULATION RESULTS

The $i_d = 0$ control strategy is adopted, and the speed loop adopts traditional PI control. The simulation time is set to 0.4s, and the given speed is 1000 r/min. Motor starts without load, and a sudden load of 3N · m is added at 0.1s. At 0.3s, the torque is suddenly applied to 6N · m. In this paper, the steady-state performance and dynamic response ability of the control system with different predictive algorithms in the case of inductance mismatch are explored, and the following simulations are carried out.

1) Traditional deadbeat predictive current control is adopted.
2) Adaptive deadbeat predictive current control is adopted.
3) Adaptive deadbeat predictive current control with feed forward control is adopted.

Firstly, performance under the condition of inductance mismatch less than 50% is explored. Considering the measurement error of motor parameters and the saturation effect of magnetic circuit, the inductance of the motor used in control strategy becomes 1.1mH, and the mismatch is less than half of the nominal inductance. Figures 3 to 5 show the response curves of the three predictive models, respectively.

Figure 3 shows the response curves of the traditional deadbeat predictive current control. It can be seen that when the

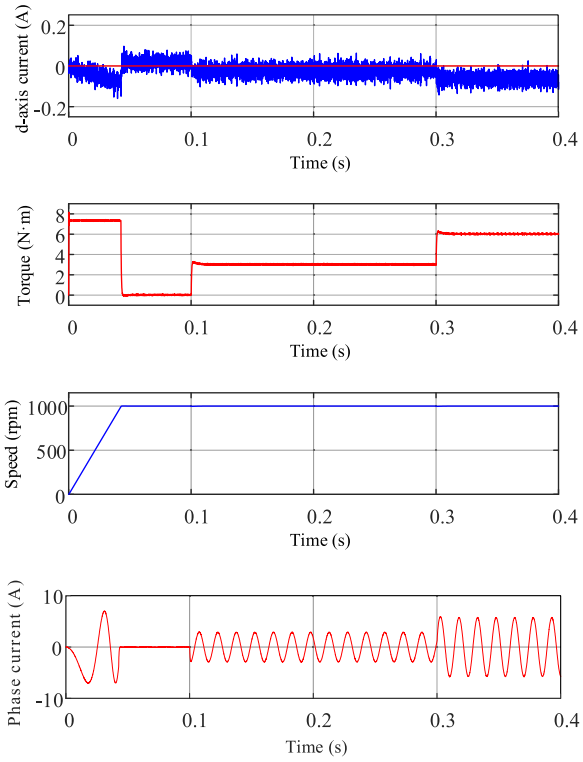

FIGURE 3. Simulation curves of traditional DPCC.

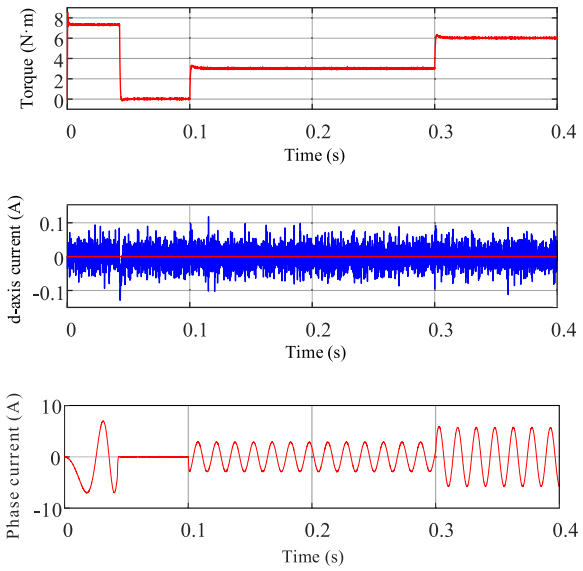

FIGURE 4. Simulation curves of adaptive DPCC.

inductance is mismatched, the current of d axis cannot follow the given value, resulting in a steady-state error and reducing the operation efficiency of the motor.

After adopting the adaptive deadbeat predictive model, the steady-state error caused by the inductance disturbance is completely eliminated, and the current of d axis can follow the given value without error. As shown in Figure 4, the system also maintains good dynamic performance.

When the inductance mismatch is minor, the steady-state error is completely eliminated by adaptive DPCC. But there

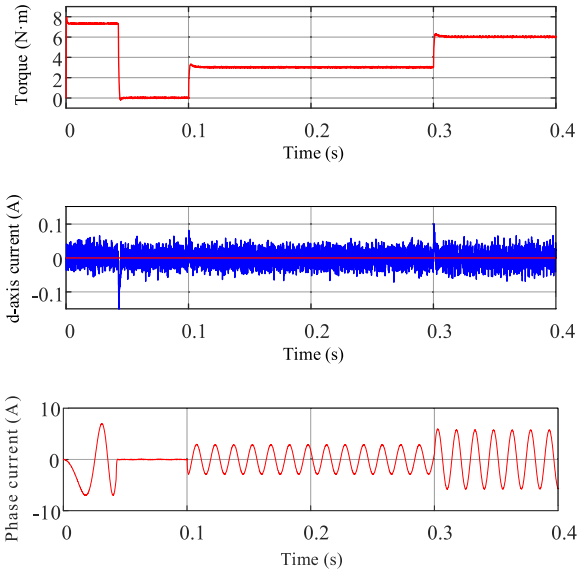

FIGURE 5. Simulation curves of adaptive DPCC with feed forward.

are problems such as large current distortion and torque ripple. After the introduction of feed forward control, as shown in Figure 5, it can be found that the distortion of current is reduced, and the harmonic is also suppressed.

When the inductance mismatch is equal to half of the nominal inductance and reaches the limit of stability margin of traditional DPCC or adaptive DPCC, the three current predictive algorithms are simulated and compared. The inductance of the motor is reduced to 0.788mH, and the response curves are shown in figures 6 to 8.

Figure 6 shows the response curves of the traditional DPCC. It can be seen that when the inductance mismatch reaches the stability margin, the system generates oscillation. The current distortion and electromagnetic torque ripple significantly increase. At the same time, the steady-state

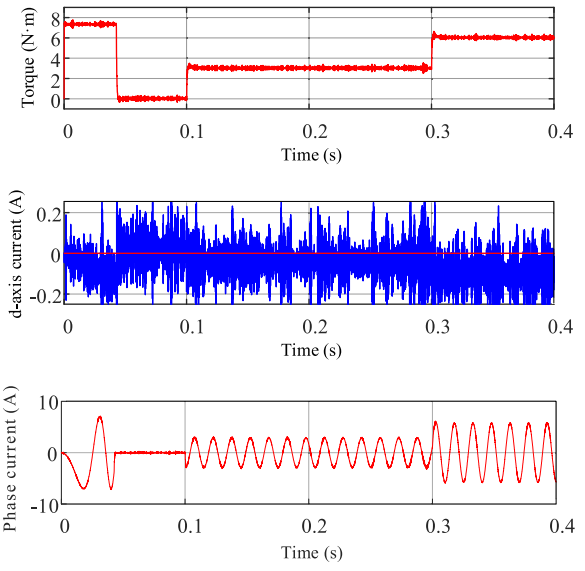

FIGURE 6. Simulation curves of traditional DPCC.

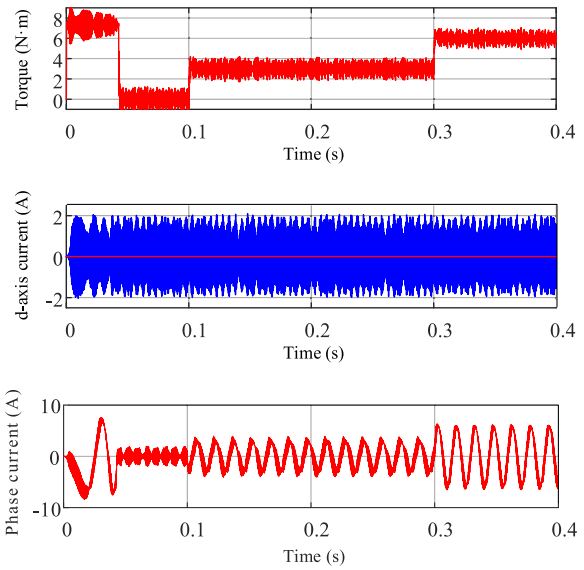

FIGURE 7. Simulation curves of adaptive DPCC.

error of d axis current cannot meet the requirement of high precision.

With the adaptive DPCC, when the inductance becomes half of the nominal, the steady-state error of d-axis current is eliminated. Due to the introduction of approach coefficients in voltage disturbance terms, severe inductance mismatch causes the increase of current and torque pulsation, and the system cannot operate stably. The response curves are shown in Figure 7.

With the introduction of feed forward control, the stability margin of the system to inductance mismatch is increased. Figure 8 shows the response curves of the adaptive DPCC with feed forward control. The improved algorithm can eliminate the steady-state error completely, reduce the current distortion and torque ripple, and ensure the dynamic performance of control system.

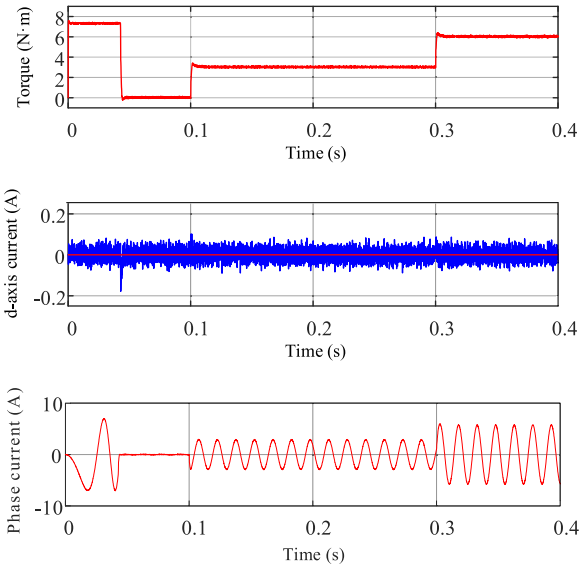

FIGURE 8. Simulation curves of adaptive DPCC with feed forward.

TABLE 2. Comparison of steady-state performance of the motor with inductance parameters=1.1mH.

Control method	Torque ripple T_{rip}(N·m)	THD	Current amplitude(A)	steady-state error
Traditional DPCC	0.0469	0.92%	5.7392	Yes
Adaptive DPCC	0.0512	1.03%	5.7389	No
Adaptive DPCC with feed forward	0.0448	0.86%	5.7389	No

TABLE 3. Comparison of steady-state performance of the motor with inductance parameters=0.788mH.

Control method	Torque ripple T_{rip}(N·m)	THD	Current amplitude(A)	steady-state error
Traditional DPCC	0.1174	2.71%	5.7464	Yes
Adaptive DPCC	0.529	26.47%	5.7348	No
Adaptive DPCC with feed forward	0.0641	1.22%	5.7456	No

The steady-state performances of the three control algorithms are further quantitatively compared. The average value of motor torque ripple in N sampling periods is calculated as follows

$$T_{rip} = \sqrt{\frac{1}{N}\sum_{i=1}^{N}(T_e(i) - T_e^*)^2} \tag{28}$$

where N is the number of sampling cycles and T_{rip} is the average torque ripple. T_e (i) is the electromagnetic torque of the i_{th} cycle and T_e^* represents the average electromagnetic torque.

When the inductance becomes 1.1mH and 0.788mH, comparisons of the steady-state performances from 0.3s to 0.4s of different predictive algorithms are shown in Table 2 and Table 3, respectively. The distortion rate of phase current is obtained by FFT analysis.

It can be seen from Table 2 that when the inductance mismatch is small, the adaptive DPCC proposed in this paper can eliminate the steady-state error and reduce the amplitude of stator current. Still, compared with the traditional DPCC, the torque ripple and current distortion rate are increased by 9.17% and 11.96%, respectively. While, after introducing feed forward control, the torque ripple and current distortions are 87.5% and 83.5% of the original, respectively. Therefore, the proposed strategy can effectively improve the steady-state performance when the inductance mismatch is slight.

When the actual inductance becomes half of the nominal, the steady-state performances of the three strategies are compared in Table 3.

It can be seen from Table 3 that when the actual inductance becomes half of the nominal, due to the introduction of the approaching coefficients in voltage disturbance terms, the torque ripple and current distortion of adaptive DPCC increase significantly, which cannot be used in the field of practical engineering. For adaptive DPCC combined with feed forward control, torque ripple and current distortions

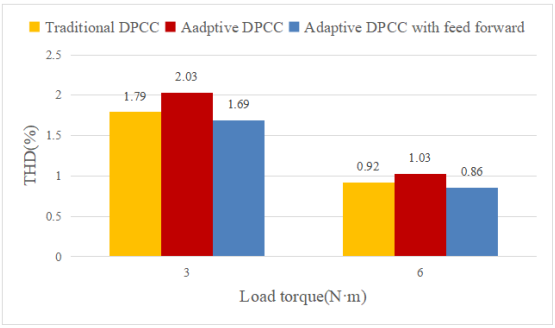

FIGURE 9. Current THD comparison between three DPCC strategies with inductance parameters=1.1mH.

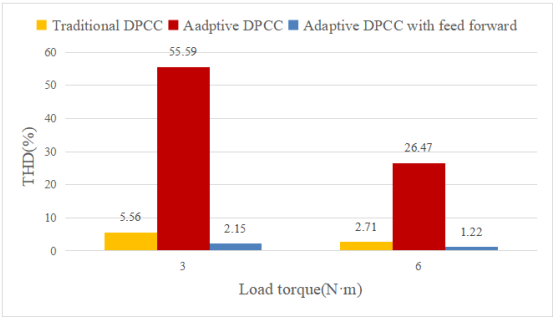

FIGURE 10. Current THD comparison between three DPCC strategies with inductance parameters=0.788mH.

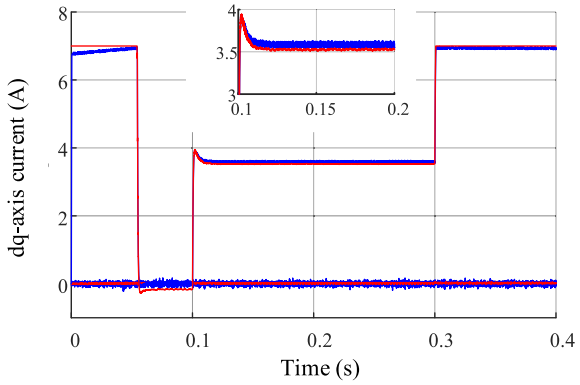

FIGURE 11. Current curves of traditional DPCC.

are greatly reduced, and the steady-state performance of the system is significantly improved.

FFT analysis is carried out for the phase currents of various strategies under different loads, and the results are shown in figure 9 and figure 10.

It is further verified that the improved model proposed in this paper can avoid the influence of resistance and flux linkage changes. Assuming that the stator resistance of SPMSM is changed to $2R_s$ and the flux linkage is reduced to 80% of the nominal due to the temperature rise, while the other operating conditions remain unchanged, the simulations are carried out. The dq-axis current response curves of three predictive models are shown in Figure 11 to 13, in which

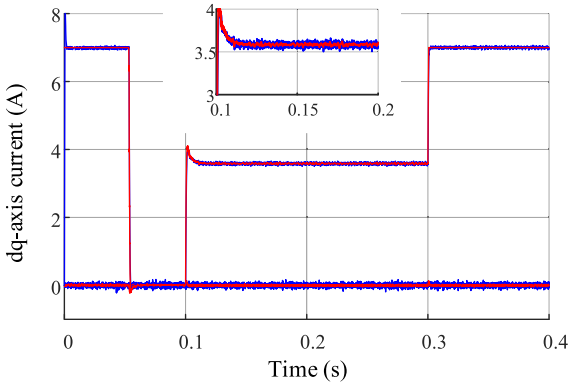

FIGURE 12. Current curves of adaptive DPCC.

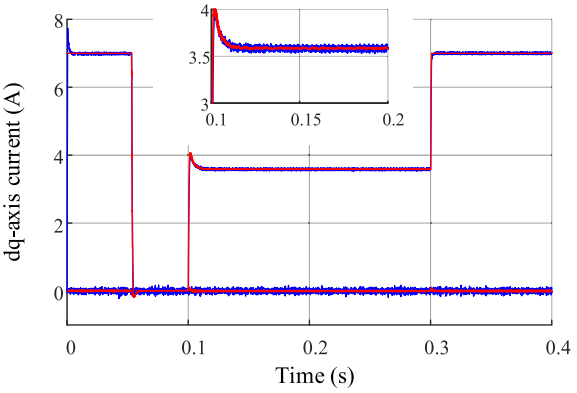

FIGURE 13. Current curves of adaptive DPCC with feed forward.

the red curve represents the given current, and the blue curve represents the actual current.

It can be seen that both the adaptive DPCC and the proposed strategy with feed forward control can eliminate the steady-state error. It shows that the adaptive model presented in this paper can avoid the influence caused by the changes of resistance and flux linkage.

B. EXPERIMENTAL RESULTS

To further verify the practicability of the above analysis, corresponding experimental tests are carried out on the SPMSM drive platform. The test bench is shown in Figure 14.

The given speed is 300 r/min, motor starts without load. After 2s, the torque is suddenly increased to 4N · m, and the speed is increased to 600 r/min when the motor runs stably. The inductance in the control algorithm is increased to simulate the actual reduction of motor inductance.

First, experiment with the operating conditions where the inductance parameter mismatch is less than 50%. Figure 15 shows the experimental curves of the traditional DPCC when the inductance becomes 1.1mH. The current is distorted, and the steady-state error of d-axis current exists. The operation efficiency is significantly reduced.

Another experiment is performed on traditional DPCC with feed forward control. The value of weight q is 0.5, and

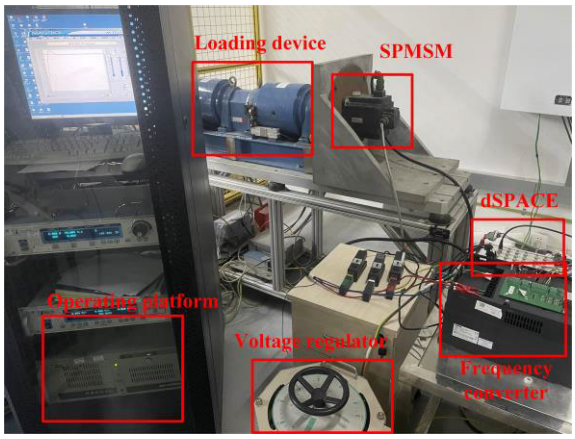

FIGURE 14. Test bench.

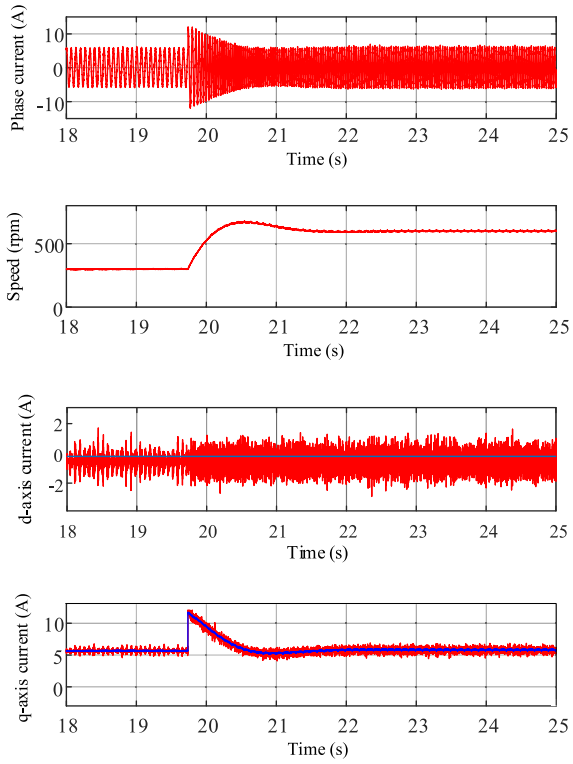

FIGURE 15. Experimental curves of traditional DPCC.

the experimental curves are shown in Figure 16. When the inductance becomes 1.1mH, the current distortion is obviously reduced, but the steady-state error is increased, which cannot meet the accuracy requirements. To sum up, the traditional methods cannot solve the problem of steady-state error when the parameters are mismatched.

Experiments are performed on the adaptive DPCC and the feed forward predictive model under the same operating conditions. The experimental curves are shown in Figure 17. The steady-state error of the d-axis current is eliminated. For the adaptive model with feed forward, the current distortion and pulsation are reduced, and the steady-state performance of the system is significantly improved.

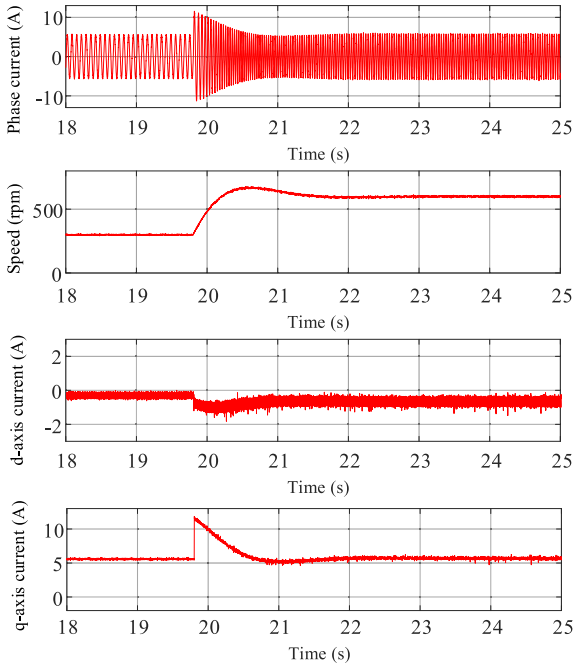

FIGURE 16. Experimental curves of traditional DPCC with feed forward.

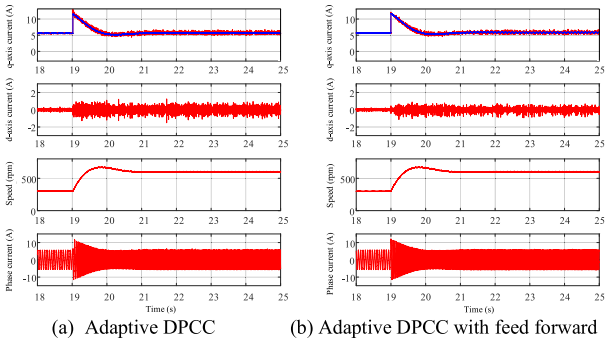

FIGURE 17. Comparison of experimental curves before and after introducing feed forward control.

Then the experiment is carried out under the condition that the mismatch of inductance is equal to 50% of the nominal. Figure 18 shows the experimental curves of adaptive DPCC. The response current is seriously distorted. The motor violently vibrates and cannot operate stably.

Figure 19 shows the experimental curves of the adaptive DPCC with feed forward when the inductance becomes half of the nominal inductance. It can be seen that the current distortion and pulsation are greatly reduced, and the steady-state performance of the system is improved obviously.

When the inductance mismatch is more than half of the nominal, experiments are carried out on adaptive DPCC with feed forward to verify the effectiveness of model proposed in this paper in increasing the allowable inductance error range for system stability. The inductance of the motor becomes 0.55mH, which is 35% of the nominal. Experimental curves are shown in Figure 20.

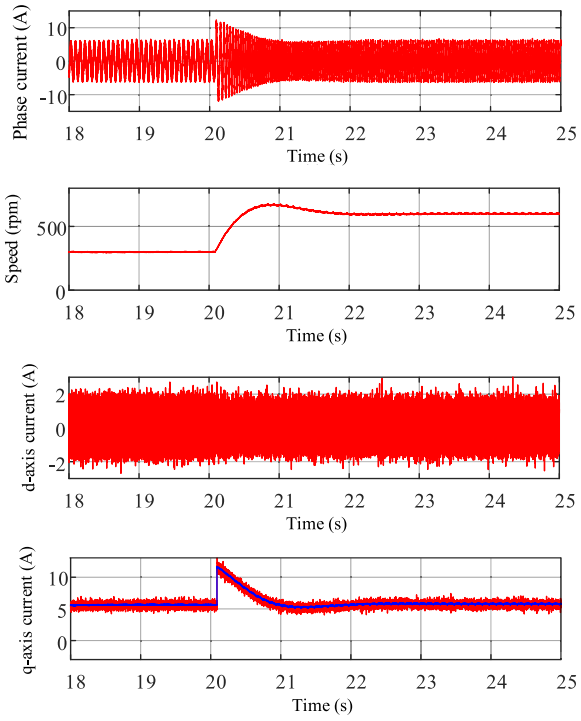

FIGURE 18. Experimental curves of adaptive DPCC when $L = 0.788$mH.

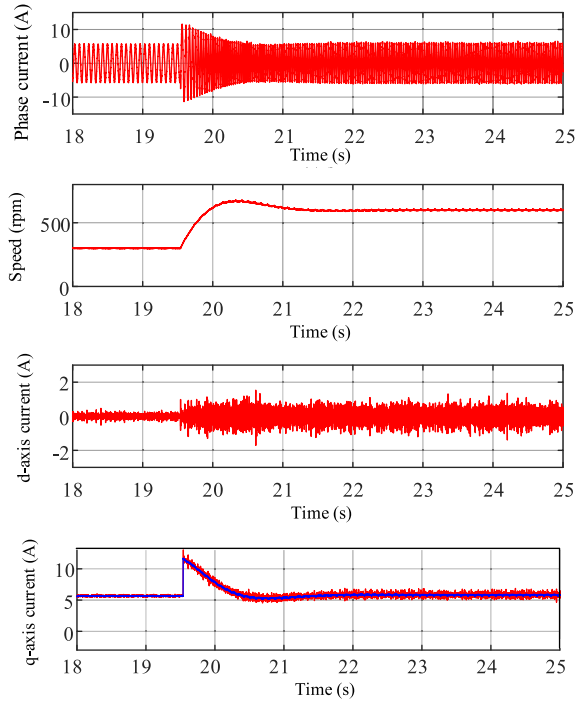

FIGURE 19. Experimental curves of adaptive DPCC with feed forward when $L = 0.788$mH.

It can be seen from Figure 20 that the proposed adaptive DPCC with feed forward can significantly improve the response performance when faced with extreme parameter mismatch conditions. The robustness and steady-state performance of the speed control system are also improved.

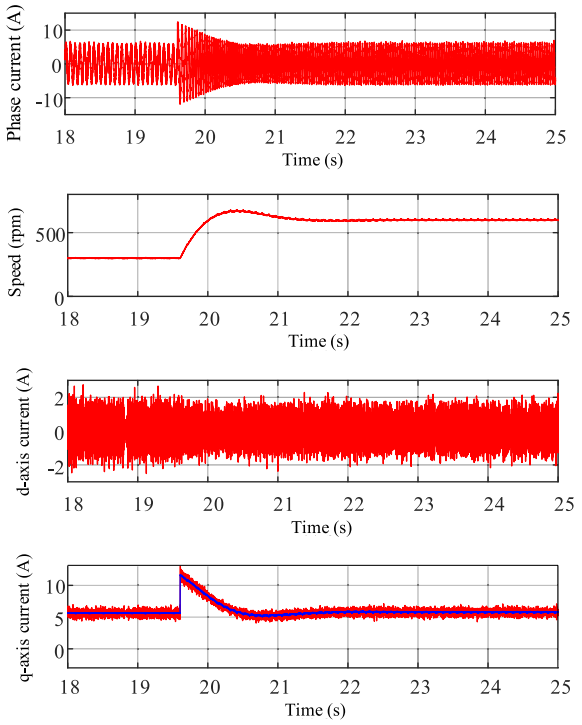

FIGURE 20. Experimental curves of adaptive DPCC with feed forward when $L = 0.55$mH.

VI. CONCLUSION

In this paper, the parameter sensitivity of DPCC for SPMSM is studied. Aiming at problems such as current steady-state error and torque ripple under conditions of motor parameter mismatch or change for traditional deadbeat control principle, an adaptive deadbeat predictive current control is proposed. The model is only related to the inductance and completely eliminates the steady-state error of the current. To expand the stability margin of the system, an adaptive DPCC scheme with feed forward is presented, which expands the critical inductance disturbance value from 50% to 67% when the system oscillates. The model presented in this paper can improve the robustness of DPCC while ensuring the response performance of the system.

REFERENCES

[1] J. Hang, H. Wu, J. Zhang, S. Ding, Y. Huang, and W. Hua, "Cost function-based open-phase fault diagnosis for PMSM drive system with model predictive current control," *IEEE Trans. Power Electron.*, vol. 36, no. 3, pp. 2574–2583, Mar. 2021.

[2] C. Gong, Y. Hu, M. Ma, L. Yan, J. Liu, and H. Wen, "Accurate FCS model predictive current control technique for surface-mounted PMSMs at low control frequency," *IEEE Trans. Power Electron.*, vol. 35, no. 6, pp. 5567–5572, Jun. 2020.

[3] F. Wang, K. Zuo, P. Tao, and J. Rodríguez, "High performance model predictive control for PMSM by using stator current mathematical model self-regulation technique," *IEEE Trans. Power Electron.*, vol. 35, no. 12, pp. 13652–13662, Dec. 2020.

[4] Y. Zhang and W. Xie, "Low complexity model predictive control—Single vector-based approach," *IEEE Trans. Power Electron.*, vol. 29, no. 10, pp. 5532–5541, Oct. 2014.

[5] Y. Han, C. Gong, L. Yan, H. Wen, Y. Wang, and K. Shen, "Multiobjective finite control set model predictive control using novel delay compensation technique for PMSM," *IEEE Trans. Power Electron.*, vol. 35, no. 10, pp. 11193–11204, Oct. 2020.

[6] Y. Wang, X. Wang, W. Xie, F. Wang, and M. Dou, "Deadbeat model-predictive torque control with discrete space-vector modulation for PMSM drives," *IEEE Trans. Ind. Electron.*, vol. 64, no. 5, pp. 3537–3547, May 2017.
[7] Y. Wang, S. Tobayashi, and R. D. Lorenz, "A low-switching-frequency flux observer and torque model of deadbeat–direct torque and flux control on induction machine drives," *IEEE Trans. Ind. Appl.*, vol. 51, no. 3, pp. 2255–2267, Jun. 2015.
[8] L. Malesani, P. Mattavelli, and S. Buso, "Robust dead-beat current control for PWM rectifiers and active filters," *IEEE Trans. Ind. Appl.*, vol. 35, no. 3, pp. 613–620, May 1999.
[9] S. Mukundan, H. Dhulipati, J. Tjong, and N. C. Kar, "Parameter determination of PMSM using coupled electromagnetic and thermal model incorporating current harmonics," *IEEE Trans. Magn.*, vol. 54, no. 11, pp. 1–5, Nov. 2018.
[10] G. Pei, J. Liu, X. Gao, W. Tian, L. Li, and R. Kennel, "Deadbeat predictive current control for SPMSM at low switching frequency with moving horizon estimator," *IEEE J. Emerg. Sel. Topics Power Electron.*, vol. 9, no. 1, pp. 345–353, Feb. 2021.
[11] P. Kakosimos and H. Abu-Rub, "Deadbeat predictive control for PMSM drives with 3-L NPC inverter accounting for saturation effects," *IEEE J. Emerg. Sel. Topics Power Electron.*, vol. 6, no. 4, pp. 1671–1680, Dec. 2018.
[12] Z. Zhang, L. Jing, X. Wu, W. Xu, J. Liu, G. Lyu, and Z. Fan, "A deadbeat PI controller with modified feedforward for PMSM under low carrier ratio," *IEEE Access*, vol. 9, pp. 63463–63474, Apr. 2021.
[13] Y. Jiang, W. Xu, C. Mu, and Y. Liu, "Improved deadbeat predictive current control combined sliding mode strategy for PMSM drive system," *IEEE Trans. Veh. Technol.*, vol. 67, no. 1, pp. 251–263, Jan. 2018.
[14] L. Rovere, A. Formentini, and P. Zanchetta, "FPGA implementation of a novel oversampling deadbeat controller for PMSM drives," *IEEE Trans. Ind. Electron.*, vol. 66, no. 5, pp. 3731–3741, May 2019.
[15] Q. Zhang, Y. Fan, and C. Mao, "A gain design method for a linear extended state observers to improve robustness of deadbeat control," *IEEE Trans. Energy Convers.*, vol. 35, no. 4, pp. 2231–2239, Dec. 2020.
[16] X. Yuan, S. Zhang, and C. Zhang, "Enhanced robust deadbeat predictive current control for PMSM drives," *IEEE Access*, vol. 7, pp. 148218–148230, Oct. 2019.
[17] X. Li, S. Zhang, C. Zhang, Y. Zhou, and C. Zhang, "An improved deadbeat predictive current control scheme for open-winding permanent magnet synchronous motors drives with disturbance observer," *IEEE Trans. Power Electron.*, vol. 36, no. 4, pp. 4622–4632, Apr. 2021.
[18] X. Sun, J. Cao, G. Lei, Y. Guo, and J. Zhu, "A robust deadbeat predictive controller with delay compensation based on composite sliding-mode observer for PMSMs," *IEEE Trans. Power Electron.*, vol. 36, no. 9, pp. 10742–10752, Sep. 2021.
[19] J. S. Lee, C.-H. Choi, J.-K. Seok, and R. D. Lorenz, "Deadbeat-direct torque and flux control of interior permanent magnet synchronous machines with discrete time stator current and stator flux linkage observer," *IEEE Trans. Ind. Appl.*, vol. 47, no. 4, pp. 1749–1758, Jul./Aug. 2011.
[20] C. Xu, Z. Han, and S. Lu, "Deadbeat predictive current control for permanent magnet synchronous machines with closed-form error compensation," *IEEE Trans. Power Electron.*, vol. 35, no. 5, pp. 5018–5030, May 2020.
[21] Y. Yao, Y. Huang, F. Peng, J. Dong, and H. Zhang, "An improved deadbeat predictive current control with online parameter identification for surface-mounted PMSMs," *IEEE Trans. Ind. Electron.*, vol. 67, no. 12, pp. 10145–10155, Dec. 2020.
[22] J. Long, M. Yang, Y. Chen, K. Liu, and D. Xu, "Current-controller-free self-commissioning scheme for deadbeat predictive control in parametric uncertain SPMSM," *IEEE Access*, vol. 9, pp. 289–302, 2021.
[23] Y. Wang, N. Niimura, and R. D. Lorenz, "Real-time parameter identification and integration on deadbeat-direct torque and flux control (DB-DTFC) without inducing additional torque ripple," *IEEE Trans. Ind. Appl.*, vol. 52, no. 4, pp. 3104–3114, Jul./Aug. 2016.
[24] K. Yin, L. Gao, R. Chen, and Z. Feng, "An improved deadbeat current predictive control with active disturbance rejection for PMSM," in *Proc. Int. Conf. Robot. Control Eng. (RobCE)*, Tokyo, Japan, Apr. 2021, pp. 41–47.

KAIXUAN YIN was born in Jiangsu, China, in 1997. He received the B.S. degree in electrical engineering from the Hebei University of Technology, Tianjin, China, in 2019. He is currently pursuing the M.S. degree in electrical engineering with Xi'an Jiaotong University.

His research interests include reliability and intelligence of electrical equipment, rare-earth permanent magnet electric machines drives with modern control theories, and digital controller using the digital signal processor implementations.

LIN GAO received the M.S. degree in electrical engineering from Xi'an Jiaotong University, Xi'an, China, in 1989.

From 1993 to 1995, she was a Visiting Scholar with Queen's University, Canada. Since 1996, she has been teaching and conducting research on electric machines and machine learning. She is currently an Associate Professor with the Institute of Electrical Machine and All-Electric Technology, Xi'an Jiaotong University. Her research interests include rare-earth permanent magnet electric machines drives, power converters, and magnetic levitation technology.

RUI CHEN was born in Jiangsu, China, in 1997. He received the B.S. degree in electrical engineering from the Hebei University of Technology, Tianjin, China, in 2019. He is currently pursuing the M.S. degree in electrical engineering with Southeast University.

His main research interests include motor control and parameters identification of interior permanent magnet synchronous motor.

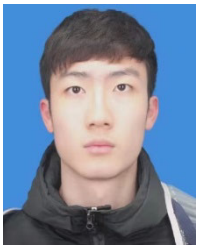

ZHIYU FENG was born in Shanxi, China, in 1998. He received the B.S. degree in electrical engineering from Xi'an Jiaotong University, Xi'an, China, in 2020, where he is currently pursuing the M.S. degree in electrical engineering.

His research interests include power converters, rare-earth permanent magnet electric machines drives with modern control theories, fault diagnosis, and fault-tolerant control.

SHEN LIU was born in Jiangsu, China, in 1995. He received the B.S. degree in electrical engineering from the China University of Mining and Technology, Xuzhou, China, in 2018. He is currently pursuing the M.S. degree in electrical engineering with Xi'an Jiaotong University.

His research interests include rare-earth permanent magnet electric machines drives with modern control theories and digital controller using the digital signal processor implementations.